Built-in skeleton Cu/NC-NFs as sulfur carrier for lithium sulfur battery

Die Su[a], Yuhong Zeng[a], Meiqi Geng[a], Tao Wang[a] * Minhua Shao[b,c], Cunpu Li[a] * and Zidong Wei[a]

[a] State Key Laboratory of Advanced Chemical Power Sources, School of Chemistry and Chemical Engineering, Chongqing University, Chongqing 400044, China.
[b] Department of Chemical and Biological Engineering, The Hong Kong University of Science and Technology, Hongkong, 999077, China.
[c] Guangzhou Key Laboratory of Electrochemical Energy Storage Technologies, Fok Ying Tung Research Institute, The Hong Kong University of Science and Technology, Guangzhou 511458, China.

Email: Tao Wang: wangtaotao@cqu.edu.cn Cunpu Li: lcp@cqu.edu.cn

Experimental Section

Synthesis of composites

Polyacrylonitrile (PAN, $(C_3H_3N)_n$, average Mw 150,000, Macklin), Aminated carbon nanotubes (CNT-NH_2, NFs, AR, XFNANO, China), N, N-Dimethylformamide (DMF, C_3H_7NO) are directly used.

The Cu/NC-NFs is synthesized in **Fig. S1**: Firstly, according to the preparation method of Zhang group, the HKUST-1 was synthesized. Secondly, 1 g PAN, 0.12 g CNT-NH_2, and 0.7 g HKUST-1 are ground evenly and dissolved in 12 mL DMF via magnetic stirring in 40°C for 5 days to obtain the precursor solution. Thirdly, the precursor solution was spun in 15 kV of voltage for 24 h, wherein the flow rate is 0.07 mm min^{-1} and the distance from the tip to the collection plate is 16 cm. The precursor nanofiber film was stabilized in N_2 atmosphere at 200°C for 100 mins, then raising the temperature to 700°C for 200 mins, and the heating rate was 10°C min^{-1}. Finally, the CNT-NH_2/HKUST-1 nanofibers (denote as Cu/NC-NFs) were obtained after natural cooling. As a comparison figure, the PAN/CNT-NH_2 nanofibers (denote as NFs) was obtained from the precursor solution without HKUST-1 adding by the above procedure.

The melt-diffusion process is fixed to allow the elemental sulfur to seep into the prepared composites. Typically, Cu/NC-NFs and sublimed sulfur (w/w=7/3) were mixed uniformly and then annealed at 155°C for 720 mins under an N_2 atmosphere. The heating rate was 5°C min^{-1}. The black sulfur-containing composite was referred to as Cu/NC-NFs/S. The NFs/S composite was prepared with the same procedure as above.

Materials characterization

The morphologies of the samples were characterized by scanning electron microscopy (SEM, *JEOL JSM-7800F*). High-resolution field emission transmission electron microscopy images and elemental mappings were obtained using HRTEM (FE-TEM, *Talos F200s*). Raman spectra were performed on a *HORIBA Jobin Yvon S.A.S inVia* Raman spectrometer system with 325 nm (*LabRAM HR Evolution*). Powder X-ray diffraction (XRD) measurements were conducted by a *SHIMADZU* XRD-6000 diffractometer with Cu K_α radiation (λ=1.5418 Å) at a range of 5-90°. The chemical compositions of the surface of the samples were analyzed using an *Thermo scientific K-Alpha* X-ray Photoelectron Spectrometer (XPS) with Al K_α sources ($h\nu$ = 1486.6 eV). Thermogravimetric analysis (TGA) was completed under an N_2 atmosphere using a *Thermo Gravimetric Analyzer* -TGA2.

Assembly of cion batteries

Regarding N-Methyl-2-pyrrolidone (NMP) as the solvents, the liquid slurry was elaborately matched by the samples (Cu/NC-NFs/S and NFs/S), Super C, and polyvinylidene fluoride (PVDF) with 8:1:1 by mass. The sulfur load was about 2.55 mg cm^{-2}. The high sulfur load was about 5.09 mg cm^{-2}. The obtained black slurry was evenly coated on a carbon paper (4X6 cm^2) collector, dried in vacuum oven in 60°C overnight, and then punched to the discs of 10 mm diameter as the working electrodes. The CR-2032 coin batteries were prepared in the argon-filled glove box in both water and oxygen below 0.1 ppm, with lithium foil as the counter/reference electrode, PP membrane (Celgard 2500) as the separator. 1.0 M lithium bis(trifluoromethyl sulfonyl)imide (LiTFSI) dissolved in the mixed solution of 1,3-

dioxane (DOL) and Dimethoxymethane (DME) (v/v=1/1) as electrolyte, and 1 *wt*% $LiNO_3$ as additive.

Electrochemical measurements

The GCD tests were carried out on a CT2001A battery system (LAND, Wuhan) in a 1.6-2.8 V voltage window at 30°C. Cyclic voltammetry (CV) curves were obtained on an electrochemical workstation (LAND M340A, China) with a scan rate of 0.1-0.5 mV s^{-1} from 1.5 to 3.0 V. Electrochemical impedance spectroscopy (EIS) data were recorded using a Solartron Metrology (Metrohm Autolab, English) impedance analysis with a ±5 mV sine wave in the frequency range of 10^6 to 0.01 Hz.

Adsorption tests of lithium polysulfides

2.5 mM Li_2S_6 solution was synthesized by dissolving sulfur and Li_2S (molar ratio=1:5) into a mixed solvent of DOL/DME (1:1 volume ratio). For the polysulfide static adsorption experiment, Cu/NC-NFs/S and NFs/S with equal amounts of 10 mg each were added to the 5 mL Li_2S_6 solution. All the above operations were carried out in a glove box filled with argon.

Li_2S nucleation/dissociation tests

0.3 M Li_2S_8 solution was prepared by dissolving sulfur and Li_2S with a molar ratio of 1:7 in a DOL/DME solution (1:1 volume ratio). Lithium foil and the prepared Cu/NC-NFs/S and NFs/S were employed as the anode and the cathode, respectively. Then the coin batteries were assembled by dropping the electrolyte containing 25 μL Li_2S_8 to the cathode side and the electrolyte containing 25 μL conventional electrolyte to the anode side. For the nucleation test of Li_2S, all assembled coin batteries were galvanostatically discharged to 2.06 V at 0.112 mA and remained potentiostatically at 2.05 V until the current gradually decreased to 0.01 mA. For the dissociation test of Li_2S, the coin batteries were firstly galvanostatically discharged at 0.01 mA to 1.80 V to completely convert the S species to solid Li_2S. Subsequently, these coin batteries were potentiostatically charged at 2.40 V to convert Li_2S to soluble lithium polysulfides until the charging current was lower than 0.01 mA.

Calculation of diffusion coefficient for Li^+

To determine the Li-ion diffusion coefficient, the corresponding peak currents are fitted according to Randles-Sevcik Equation (1):

$$I_p = 269000 n^{1.5} \mathrm{A} C D^{0.5} v^{0.5} \quad (1)$$

Where the I_P is CV peak current, n is the electron transfer number in the redox process, A is the area of electrode (cm^2), C is the Li-ion concentration participating in redox reaction (mol cm^{-3}), D is the ion diffusion coefficient (cm^2 s^{-1}), v is the scan rate (v s^{-1}) set by CV. Here, n, A, and C are constants, linearly plot I_p versus $v^{1/2}$, the slope obtained is the Li-ion diffusion rate.

NTR equation calculation

The electron transfer per second of peak C1 (C_{e1}) and peak C2 (C_{e2}) can be obtained by integral area and scan rate:

$$C_e = \frac{A_t}{v} \quad (2)$$

C_e refers to the electron transfer amount per gram (A s), A_t denotes the integral area (A V) of peak C1 and peak C2, and v is the scan rate (V s^{-1}). And the Nucleation Transformation Ratio (NTR):

$$NTR = \frac{C_{e2}}{C_{e1}} \quad (3)$$

can be calculated to evaluate the kinetic behavior of solid-liquid-solid cascade reaction. Calculated from electronic gains and losses, NTR is theoretically close to 3.

The lattice mismatch calculation

The lattice constants for cubic structure of Cu ($Fm\bar{3}m$) are a=b=c=3.58 Å. While for Li_2S, which also exhibits a cubic structure ($Fm\bar{3}m$), the lattice constants are a=b=c=5.67 Å. The same crystal group allows for a suitable lattice match. The lattice mismatch (f) between Cu and Li_2S can be calculated using the following equation:

$$f = (\alpha_s - \alpha_g)/\alpha_s \quad (4)$$

Where the α values represent the lattice constants. For instance, taking the a-axis as an example, the lattice parameter for α_s (Cu) is 17.90 Å (calculated as 3.58 × 5), and for Li_2S, it is α_g is 17.01 Å (calculated as 5.67 × 3). This results in a low *f* of approximately 5%.

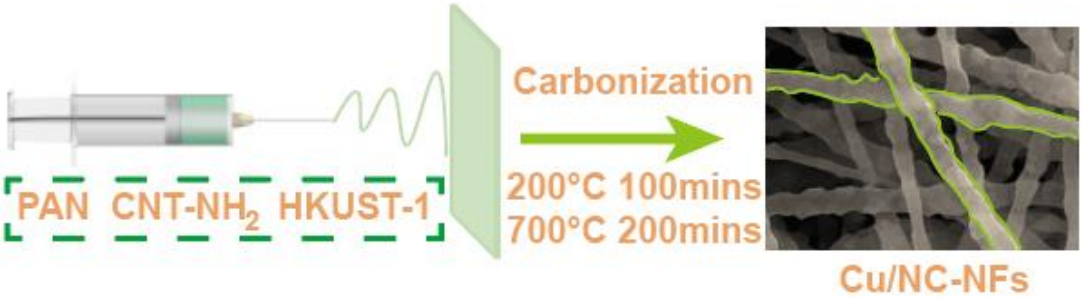

Fig. S1 Schematic diagram of preparation the Cu/NC-NFs.

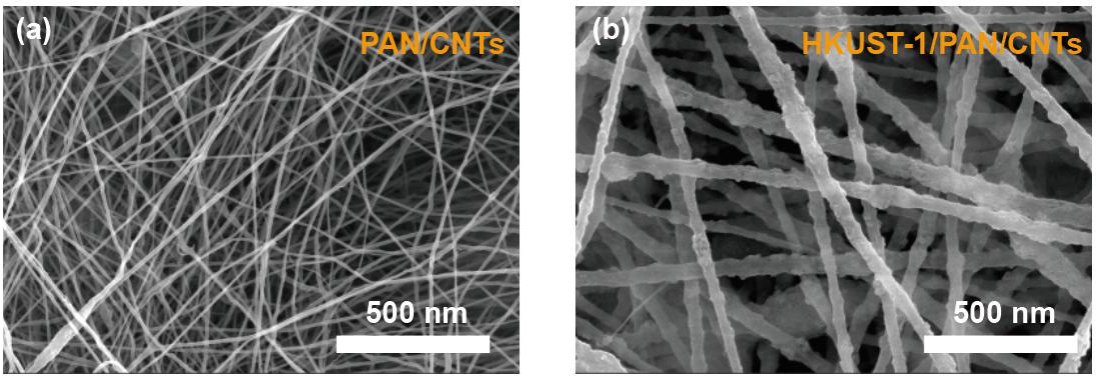

Fig. S2 SEM images of (a) precursor nanofibers of NFs, and (b) precursor nanofibers of Cu/NC-NFs.

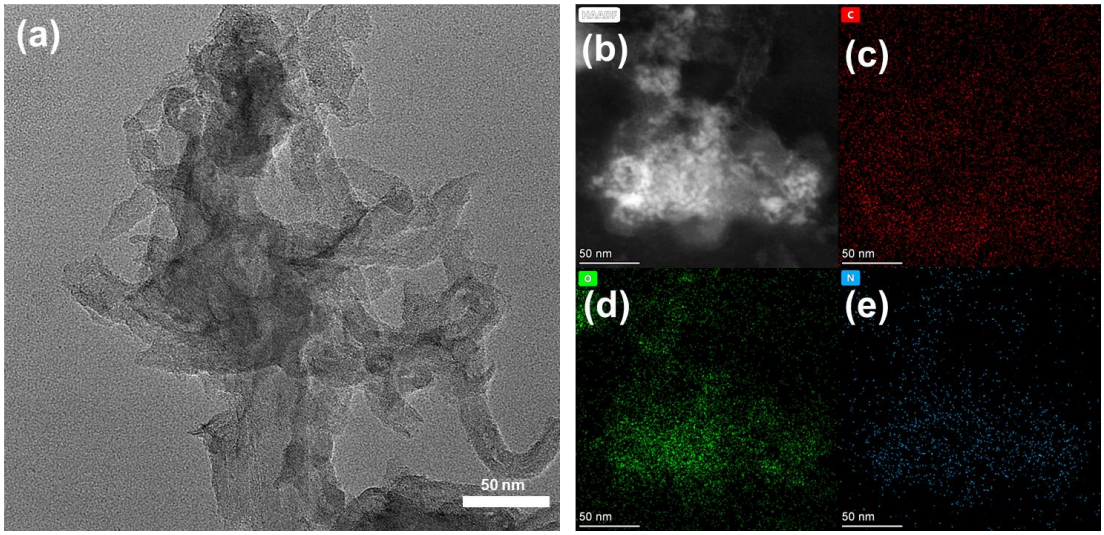

Fig. S3 (a) FE-TEM and (b)~(e) elemental mapping images of C, O, N of NFs.

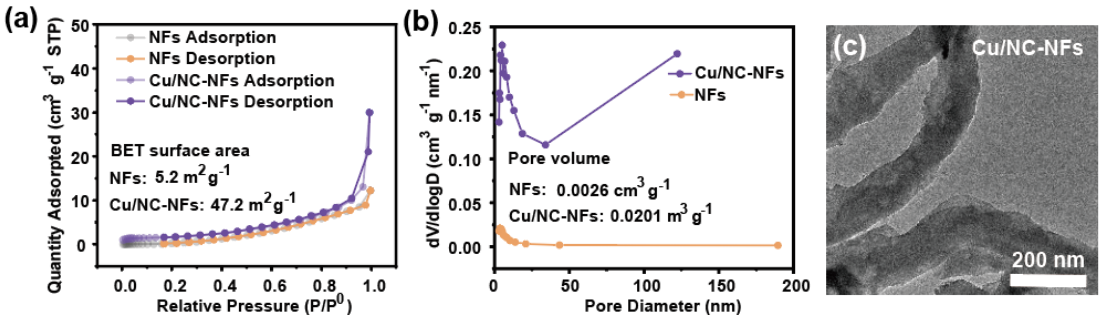

Fig. S4 The N_2 adsorption-desorption tests for NFs and Cu/NC-NFs: (a) the BET surface area and (b) the pore size distribution. (c) the TEM images for Cu/NC-NFs.

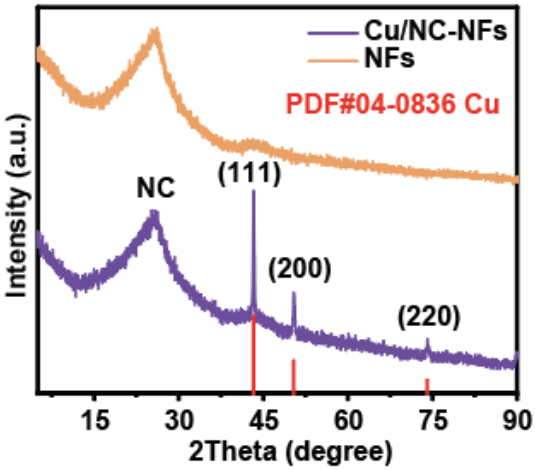

Fig. S5 XRD patterns of Cu/NC-NFs and NFs.

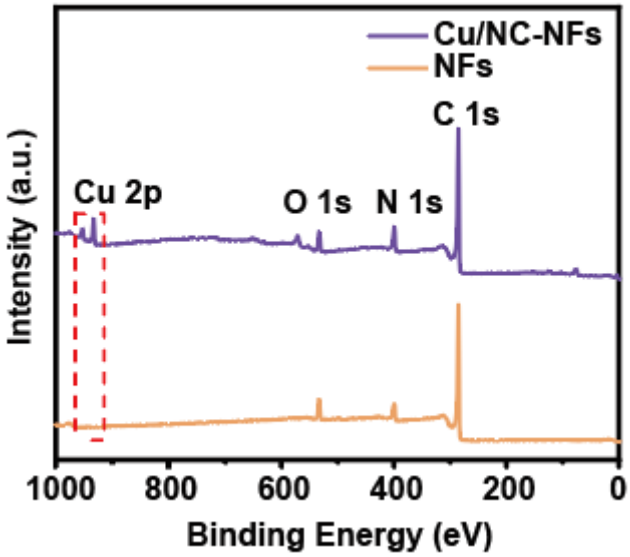

Fig. S6 XPS survey spectra for Cu/NC-NFs and NFs.

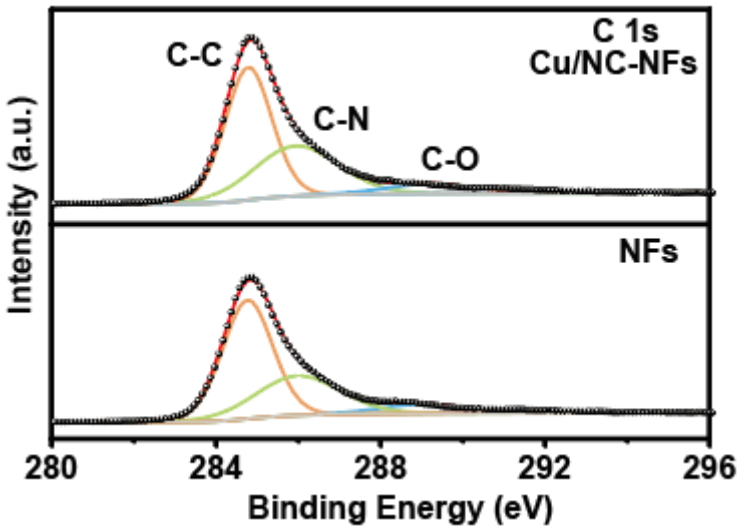

Fig. S7 The high-resolution C *1s* of Cu/NC-NFs and NFs.

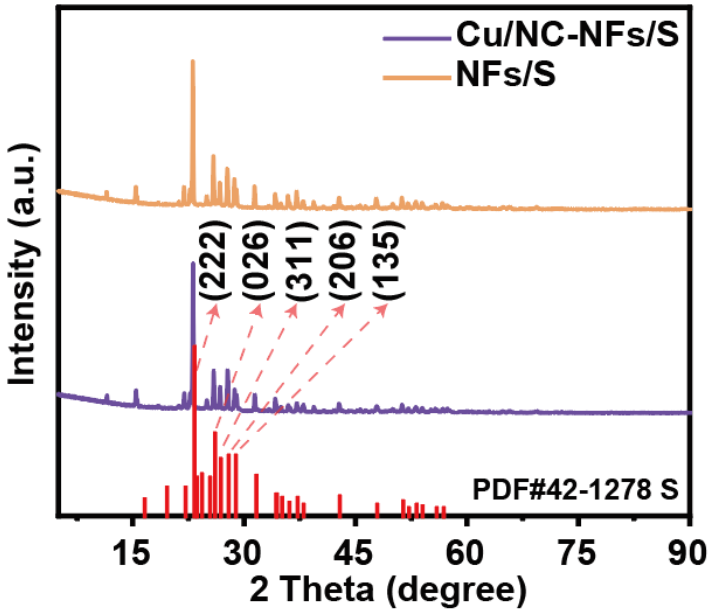

Fig. S8 The XRD patterns of the Cu/NC-NFs/S electrode and the NFs/S electrode.

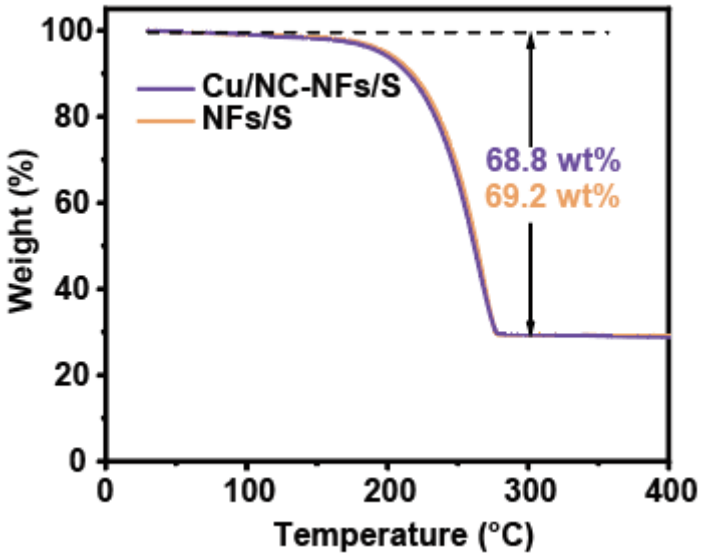

Fig. S9 TG curves for Cu/NC-NFs/S and NFs/S.

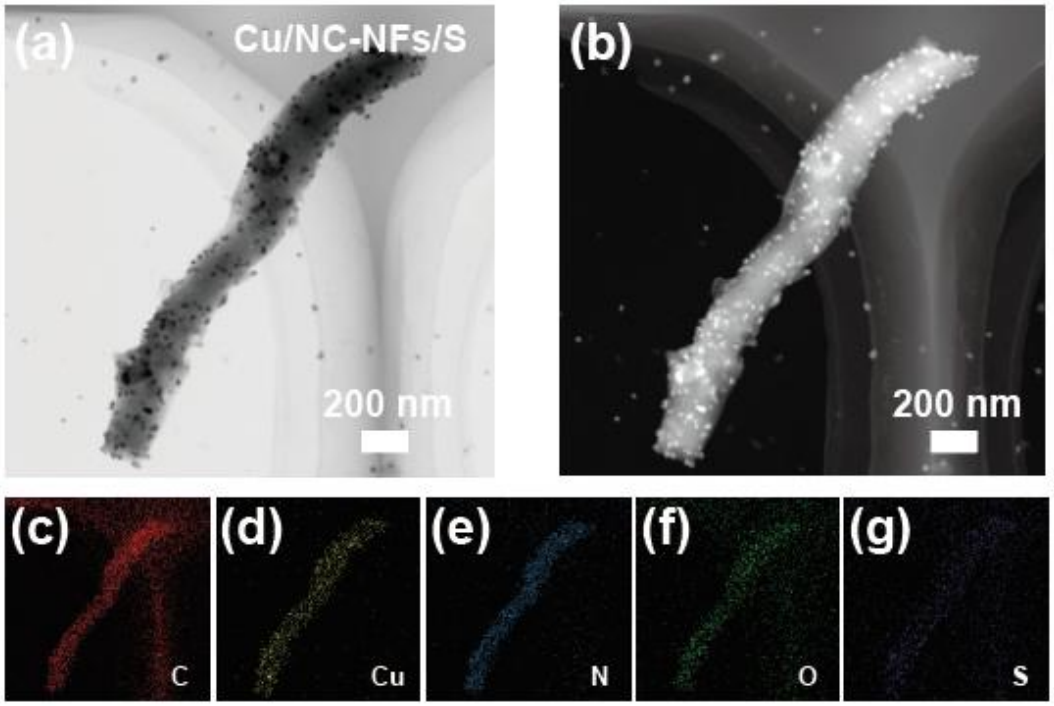

Fig. S10 The Cu/NC-NFs/S: (a) TEM image, (b) STEM image, (c-g) the mapping images of C, Cu, N, O, and S. According to the TEM/STEM images for Cu/NC-NFs/S, the results show that the nanofibers are significantly enriched with S due to their suitable pore structure. The mapping results show that the C, Cu, N, O, and S elements are evenly distributed in the fibers.

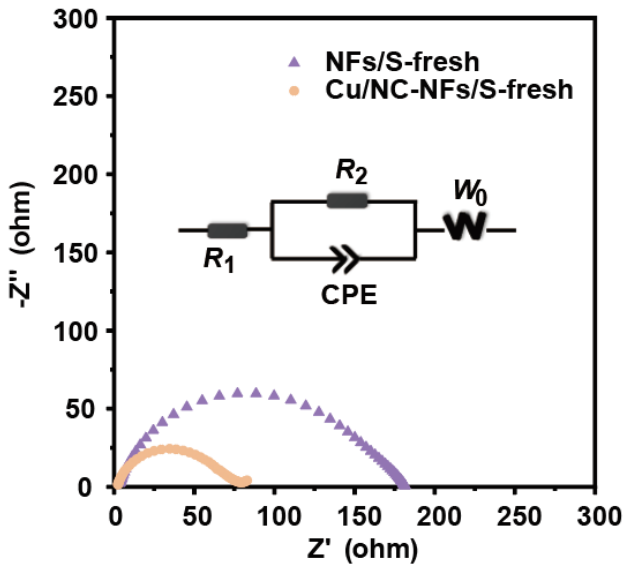

Fig. S11 Nyquist plots of NFs/S and Cu/NC-NFs/S electrodes with an inset showing the equivalent circuit diagram.

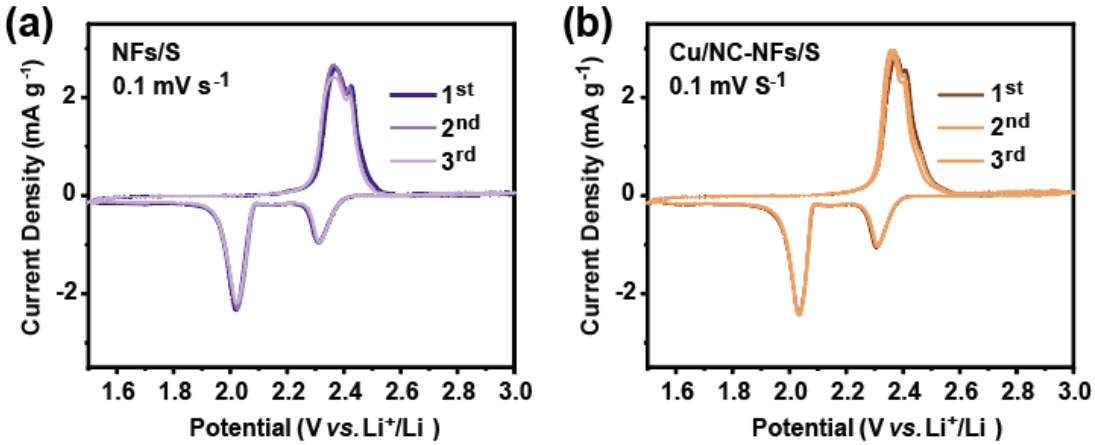

Fig. S12 The CV curves of the first three curves of (a) the NFs/S and (b) the Cu/NC-NFs/S electrode at scan rate of 0.1 mV s^{-1}. CV curves in 0.1 mV s^{-1} at first three loops reveal better overlap for Cu/NC-NFs/S, demonstrating superior cycling stability compared to NFs/S.

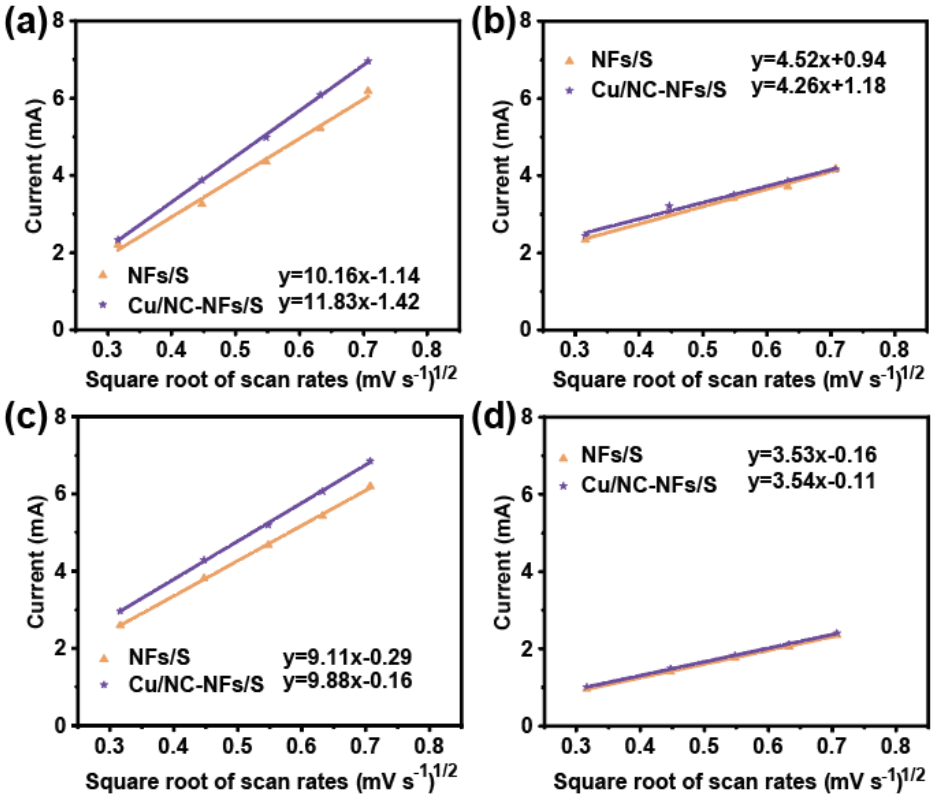

Fig. S13 I_p *vs.* $v^{1/2}$ fitting curves of the Cu/NC-NFs/S and the NFs/S electrode of (a) C1, (b) C2, (c) A1, (d) A2.S

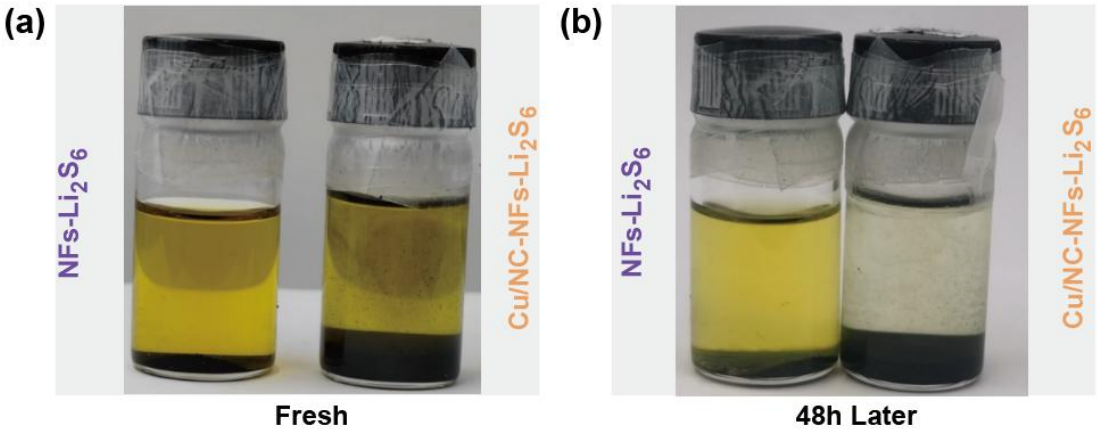

Fig. S14 Digital photos of adsorption experiment for LiPSs for (a) NFs/S and (b) Cu/NC-NFs/S electrodes.

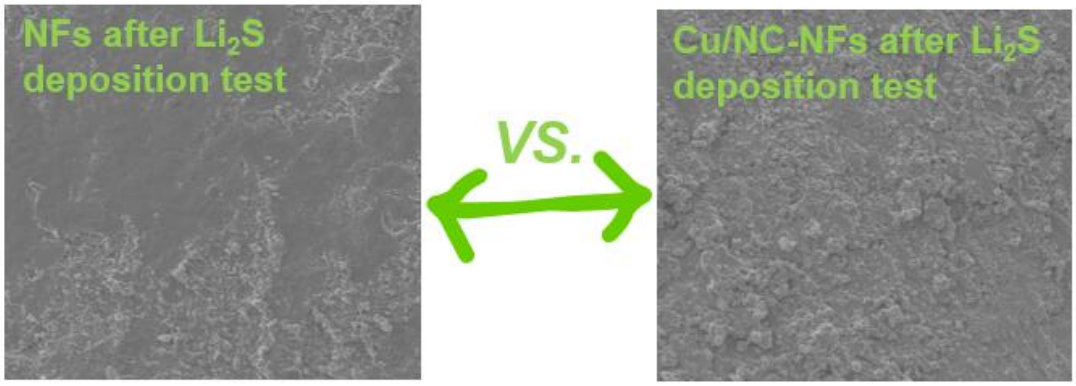

Fig. S15 The SEM images of NFs (left) and Cu/NC-NFs (right) after Li_2S deposition test.

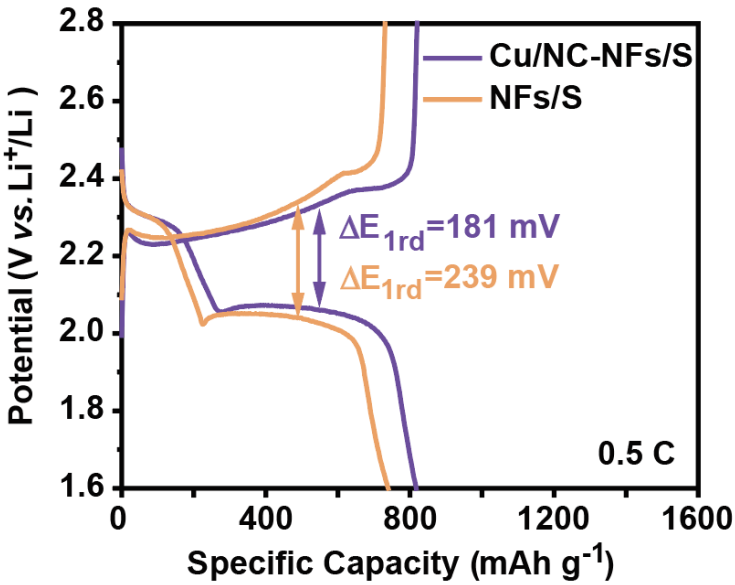

Fig. S16 Compare the overpotential values of electrodes at first cycle.

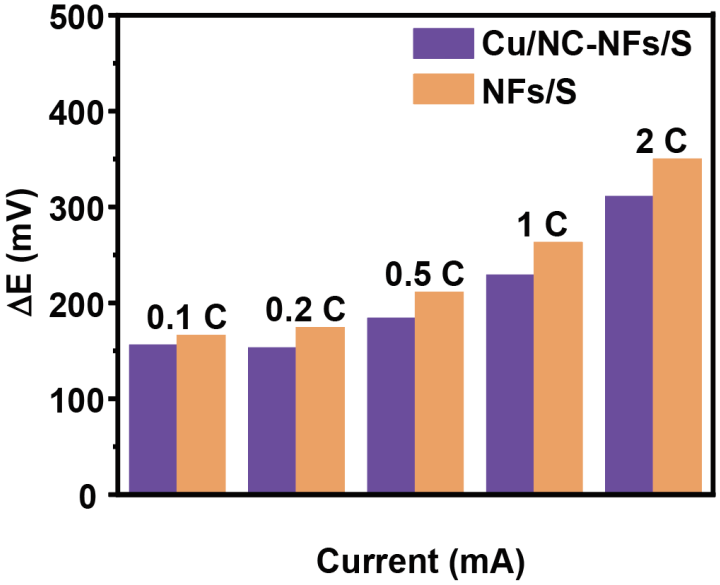

Fig. S17 Cycling performance of Cu/NC-NFs/S and NFs/S electrode corresponding charging/discharging median potential difference diagram.

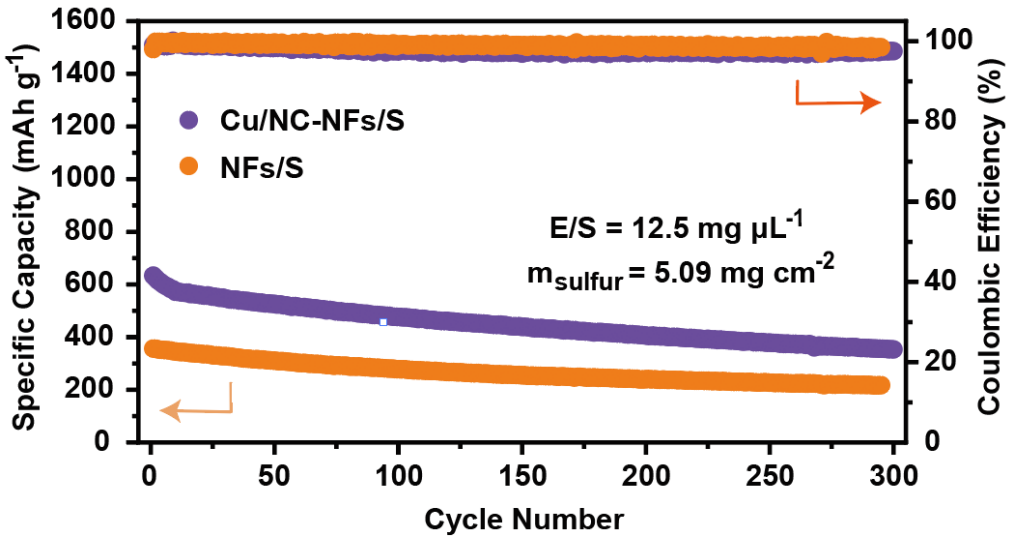

Fig. S18 Cycling performance of NFs/S and Cu/NC-NFs/S cathode with a sulfur loading of 5.09 mg cm^{-2} at 2 C.

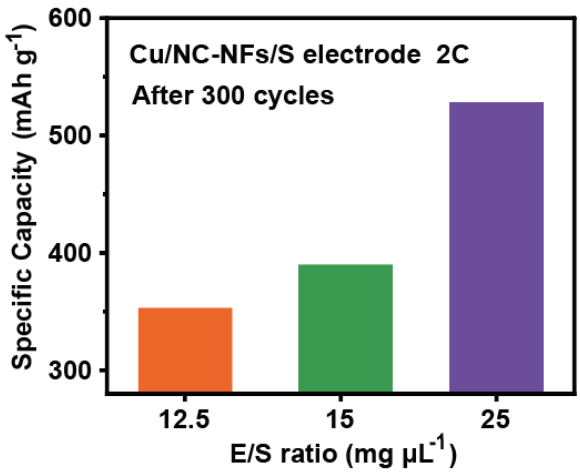

Fig. S19 Cycling performance of Cu/NC-NFs/S cathode with a different E/S ratio at 2 C.

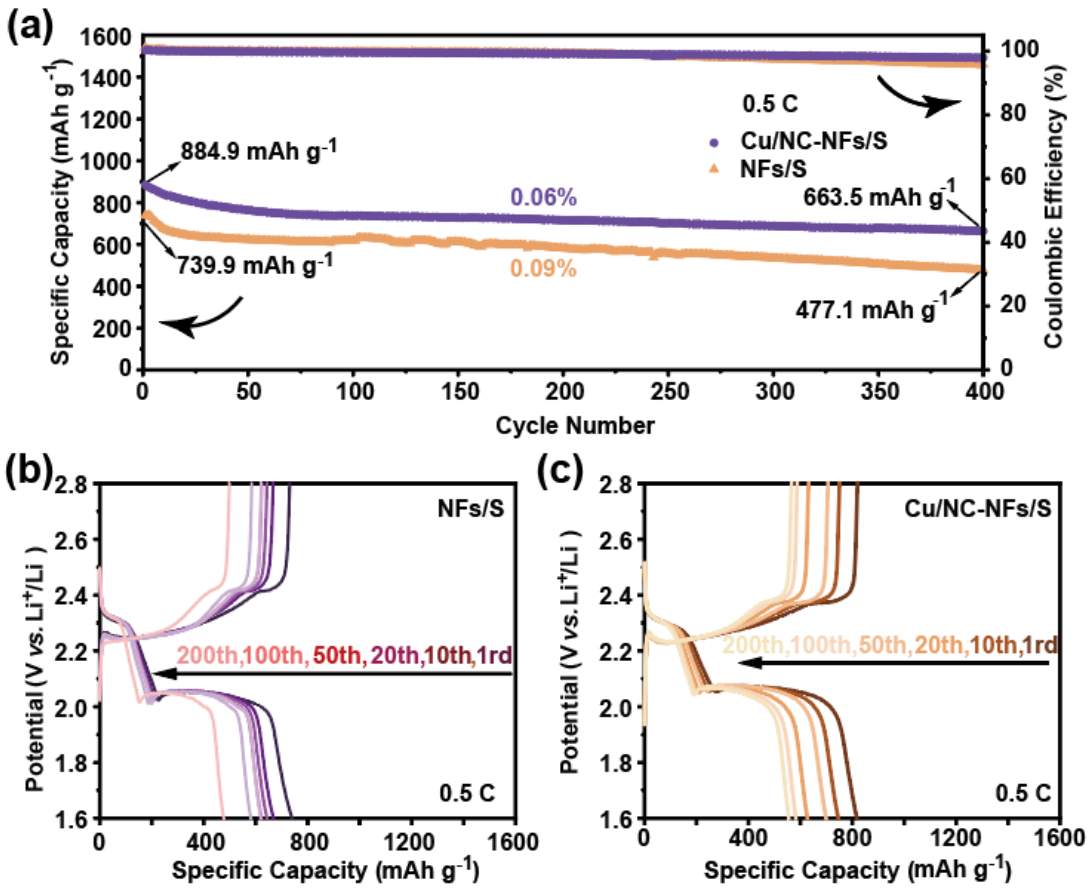

Fig. S20 Cycling performance and corresponding GCD curves of (a) the NFs/S electrode and (b) the Cu/NC-NFs/S electrode at long cycling at 0.5 C.

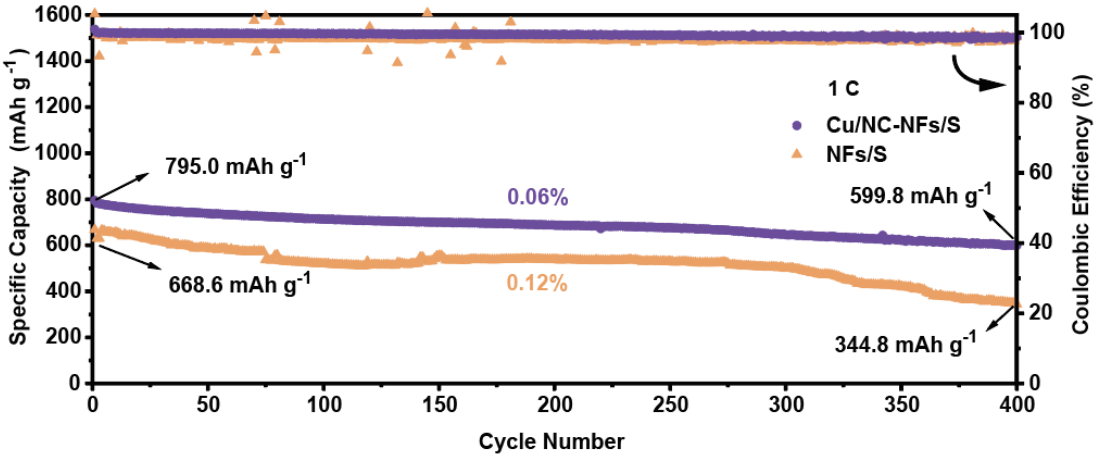

Fig. S21 The cycle performance of the Cu/NC-NFs/S electrode and the NFs/S electrode at 1 C.

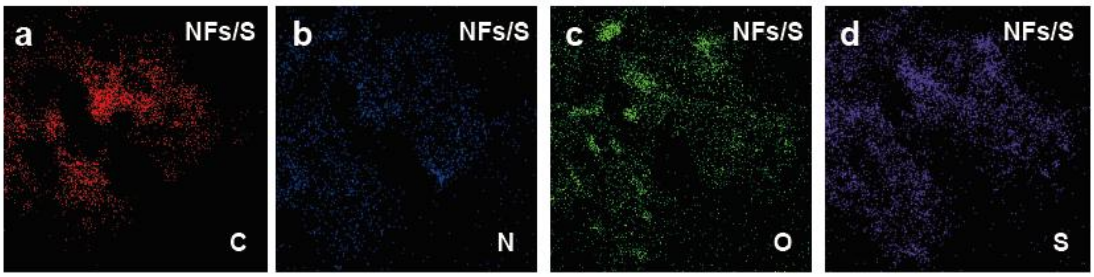

Fig. S22 (a-d) The elements mapping of C, N, O, and S for NFs/S cathode after 400 cycling.

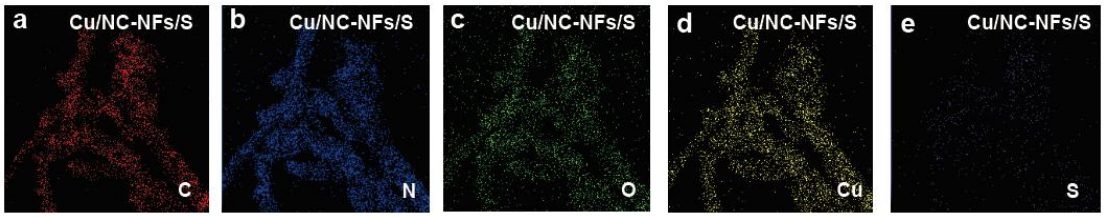

Fig. S23 (a-e) The elements mapping of C, N, O, Cu, and S for Cu/NC-NFs/S cathode after 400 cycling.

Table S1 The element content of Cu/NC-NFs.

Element	Atomic Fraction (%)	Mass Fraction (%)
Cu	2.83	13
C	80.58	70
N	9.50	9
O	7.09	8

Table S2 Simulative datum for fresh assembled coins with the Cu/NC-NFs/S electrode and the NFs/S electrode.

Samples	R_1 (Ω)	R_2 (Ω)
the NFs/S electrode	2.90	178.94
the Cu/NC-NFs/S electrode	1.88	76.93

Table S3 Recently reported electrochemical performance of Li-S battery for carbon nanofibers as sulfur carries.

Sulfur carries	Discharge specific capacity /mAh g^{-1}	Rate/C	Cycling performance	Reference
TiO_2@NCNF/S	800	0.5	150	Nano Res. 2024, 17, 1473
Ni-NCs/S	950	0.1	500	ACS Appl. Mater. Interfaces 2023, 15, 2, 3037
pCNF/S	878.8	1	1000	J. Energy Chem. 2024, 92, 619
Nb-SAs@3DOP-C/S	1208.1	0.2	100	Appl. Catal. B-Environ. 2024, 351, 124012
CNF/Co-Co_9S_8-NC/S	560.1	2	300	J. Mater. Chem. A, 2023, 11, 5212
Fe-Ni-HPCNF/S	1068.8	0.5	200	J. Colloid Interface Sci. 2023, 640, 908
TiN@CPAN/S	896	1	1000	ACS Appl. Mater. Interfaces 2023, 15, 44, 51241
Cu-CNF/TiN/S	913	2	300	Carbon energy 2024, 6, 6, e450

CoP-CoP/NPCNFs/S	1322.86	0.05	695	Appl. Catal. B-Environ. 2024, 357, 124289
Fe-SAC/S	800	1	500	Chem. Eng. J. 2023, 477, 146977
CoFe2O4/ANF/S	940	0.2	450	Chem. Eng. J. 2024, 481, 148374
NiO-MoS_2@CNFs/S	1196	0.2	100	Small 2023, 47, 19, 2304131
NiS/NiS@NCNF/S	1212.8	0.2	100	Appl. Surf. Sci. 2024, 651, 159218
Cu/NC-NFs/S	1122.2	0.1	400	*This work*